Protective Effect of Cashew Gum Nanoparticles on Natural Larvicide from *Moringa oleifera* Seeds

Haroldo C. B. Paula,[1] Maria L. L. Rodrigues,[1,2] Wesley L. C. Ribeiro,[2] Andre S. Stadler,[2] Regina C. M. Paula,[3] Flavia O. M. S. Abreu[1]

[1]*Department of Analytical and Physical Chemistry, Federal University of Ceará, Fortaleza, CE, Brazil*
[2]*Christus Research Department, Christus High School, Fortaleza-Ceará, Brazil*
[3]*Department of Organic and Inorganic Chemistry, Federal University of Ceará, Fortaleza, CE, Brazil*

Received 21 December 2010; accepted 6 July 2011
DOI 10.1002/app.35230
Published online 21 October 2011 in Wiley Online Library (wileyonlinelibrary.com).

ABSTRACT: Nanoparticles (NPs) have been used as carriers and as protective coatings of labile substances with applications in pharmacy, medicine, and agriculture. This work focused on the development of an entrapment process for the protection of a natural larvicide extracted from *Moringa oleifera* (MO) seeds with cashew gum (CG) NPs as a wall material. CG–MO NPs were characterized with regard to their size, morphology, kinetic release, thermal properties, and *Stegomya aegypti* larvae mortality. The result showed that the CG–MO NPs presented average particle sizes ranging from 288 to 357 nm, with unimodal distribution. MO larvicide active principle loading varied from 2.6 to 4.4%, and the entrapment efficiencies were in the range 39.1–60.8%. *In vitro* release kinetics showed a Fickian diffusional behavior. The thermal stability of the CG–MO NPs was related to the MO content, where their decomposition temperatures decreased with increasing MO active principle loading. Bioassays with third instar larvae showed that the mortality rate was related to larvicide loading and reached values up to 98 ± 3% mortality. The CG–MO NPs showed effective extract entrapment, with satisfactory larvicide effects even after 55 days of sample preparation and were effective as an improved and controlled release larvicide system. © 2011 Wiley Periodicals, Inc. J Appl Polym Sci 124: 1778–1784, 2012

Key words: biopolymers; drug delivery systems; nanoparticle; particle size distribution; thermogravimetric analysis (TGA)

INTRODUCTION

Nanoparticles (NPs) of natural polymers have been used extensively for the controlled release of bioactive substances, with applications in many technical areas encompassing the medical, pharmaceutical, chemical, and agricultural fields.[1–7] Besides their physicochemical properties, biodegradability, and biocompatibility, natural polymers are usually abundant and less expensive than other materials; this makes them an interesting object of investigation. Belonging to the class of natural polymers, polysaccharides have been proposed as active compound carriers for several substances. In particular, Brazilian gums, such as cashew nut gum, are branched and hydrophilic polysaccharides with high molar masses whose properties have been fully investigated.[8,9] Cashew gum (CG) is an exudate from *Anacardium occidentale* trees (cashew trees) from the Brazilian northeast and is composed of D-galactose (72%), D-glucose (14%), and arabinose (4.6%) and also contain rhamnose (3.2%) and glucuronic acid (4.7%). The main chain is formed by 1-3-linked β-D-galactose units, with the other sugars being present in polysaccharide branches.

CG has been used for several applications, including a polyacrylamide hydrogel component,[10] a polyelectrolyte complex with chitosan,[5] and as a polymeric matrix for the delivery of drugs and insecticides.[7]

Controlled delivery systems have the ability to reduce the amount of active compound in the target site, reducing the chance for toxicity and collateral damage and, thus, enhancing the bioactive substance efficiency. These systems can also be applied in the agricultural field, where pesticides can be entrapped in the polymeric matrix to maximize their effect at low concentration.[5,11] Currently, most insecticides are nonselective and can be harmful to other organisms and to the environment.[12] An alternative for the use of chemical pesticides is the utilization of natural products from plants;[13–16] this may result in more viable socioeconomic and environmental systems. *Moringa oleifera* (MO)[17–21] is a tropical tree native to the sub-Himalayan region of northwest India, and it is nowadays easily found in the Brazilian northeast region. Aqueous crude extracts and

Correspondence to: H. C. B. Paula (hpaula@ufc.br).
Contract grant sponsors: CNPQ - Conselho Nacional de Desenvolvimento Cientifico e Tecnologico; FUNCAP - Fundação Cearense de Pesquisa; INOMAT - Instituto Nacional de C,T& I em Materiais Complexos Funcionais; NANOGLYCOBIOTECH-Nanotecnologia e Biotecnologia.

essential oil of MO have been investigated and have shown antimicrobial,[20] anti-inflammatory, antispasmodic, and diuretic properties.[18] Some studies have also revealed an anticancer potential of biologically active compounds extracted from MO extract.[21,22] The aqueous seed extract has been found to contain 4-(α-L-rhamnosiloxy) benzyl isothiocyanate as the main active chemical compound.[19,23–25]

Ferreira et al.[15] demonstrated that the water extract of MO seeds showed lethal action against *Stegomya aegypti* larvae and low toxic effects on laboratorial animals. The isolation of lectins from MO aqueous extract has been described;[22,26–28] Coelho et al.[27] reported larvicidal activity and a delay of larval development due to the ingestion of lectins isolated from MO aqueous extract, which has been shown to be easily degraded.

In this work, a new system is proposed for the protection and preservation of MO active substances present in its aqueous extract through entrapment in CG NPs, with the aim of evaluating its potential for use as a new tool for dengue control. The proposed process is an alternative to those that use troublesome procedures of isolation and purification of active compounds.

EXPERIMENTAL

Materials and methods

CG from Ceará native trees (molar mass = 1.1×10^5 g/mol) was purified as described in a previous work.[8] MO seeds were collected in Fortaleza, State of Ceará, Brazil. Acetone was purchased from Synth Co. (Brazil) and was used without further purification.

Preparation of the MO seed extract

MO seeds (200, corresponding to 42.6 ± 1.1 g) were peeled and ground for 30 min in a vessel containing acetone to remove lipid components. Afterward, the acetone was removed by filtration and evaporation, and an equivalent amount of distilled water was added to the smashed seeds, which were then homogenized for 45 min, kept in refrigerator for 24 h, centrifuged, and filtered to remove any precipitated residue. This procedure was found to eliminate the most protein and lectin present in the supernatant. The aqueous extract had a density and solid content of 1.014 ± 0.002 g/cm^3 and 12.5 ± 0.3%, respectively (Table I).

TABLE I
Equivalent Amount and Seed Weight, Density, and Solid Content of the Final MO Aqueous Extract

Number of seeds	Weight (g)	Aqueous extract density (g/cm^3)	Extract solid content (%)
200	42.6 ± 1.1	1.014 ± 0.002	12.5 ± 0.3

Preparation of the CG–MO NPs

A 2% (w/v) CG aqueous solution was prepared, and the CG–MO NPs were obtained by the addition of this solution to the MO extract in different CG–MO volume ratios (3 : 1, 2 : 1, and 1 : 1). The mixture was homogenized in an Turratec ultrahomogenizer (Micronal, Brazil) for 2 min at 18,000 rpm. The resulting solution was processed in a Mini Spray Dryer B-290 (Büchi, Switzerland). The inlet and outlet air temperatures were maintained at 160 ± 5 and 65 ± 5°C, respectively, with a feed flow of 6 mL/min, an aspirator volume flow of 35 m^3/h, and an air volume flow of 84 L/h. The operational yield for all samples (white powders) was 70%.

The aqueous MO extract, without CG, was also spray-dried under the aforementioned conditions, with the aim of evaluating its properties with regard to the larvicidal activity and ζ potential data in comparison to those of the MO entrapped samples.

NP characterization

The CG–MO NPs were characterized by the Fourier transform infrared spectroscopy in a Shimadzu FTIR-8300 (Japan) spectrometer with KBr pellets. The particle size, distribution, and ζ potential were determined in a nanozetasizer (Malvern, Model Zen 3500, USA). The MO active principle loaded in the CG–MO NPs was evaluated through absorbance readings in an ultraviolet–visible spectrometer (model B582, Micronal, Brazil) at 214 nm. This wavelength was the maximum absorbance for the MO extract investigated and was in good agreement with data reported by Souza et al.,[19] according to whom the compound 4-(α-L-rhamnosiloxy) benzyl isothiocyanate absorbs at this wavelength. A calibration curve of the MO extract was built, and its equation is shown as follows:

$$\begin{aligned}\text{Absorbance} &= 6.6837 \times \text{MO active principle concentration} + 0.1191 \\ \text{correlation coefficient } R^2 &= 0.9875\end{aligned} \quad (1)$$

The MO entrapment efficiency (EE) was determined with the following equation:

$$\text{EE}\,(\%) = M/M_0 \times 100 \quad (2)$$

where M is the concentration of MO active principle in the loaded sample, as determined from eq. (1), and M_0 is the MO initial concentration in the extract.

The thermal properties of the NPs were evaluated by thermogravimetric analysis (TGA) in a Shimadzu model TGA-50 (Japan) with an N_2 atmosphere, a heating rate of 10°C/min, and a temperature range from 25 to 900°C and by differential scanning calorimetry (DSC) in a Shimadzu model DSC-50 (Japan) with a heating rate of 10°C/min from 25 to 400°C.

In vitro release

In vitro MO release was evaluated by placement of a sealed dialysis bag with 10 mL of distilled water and 50 mg of the sample into a beaker containing 200 mL of distilled water. An aliquot (1 mL) of the release medium was withdrawn at predetermined time intervals, and an equivalent amount of water replaced the solution. The aliquots of 1 mL were diluted to a total volume of 3 mL and analyzed in an ultraviolet–visible spectrophotometer at 214 nm model B582, Micronal (Brazil).

Bioassays

In vivo experiments were conducted as reported by Paula et al.[7] and can be briefly described as follows: NPs (50 and 75 mg) were placed in a beaker containing 50 mL of water and 20 second and third instar *S. aegypti* larvae, which were provided by the Ceará State Health Secretary. The larvae population was determined after 24 and 48 h by the count of dead specimens, which were subsequently removed. A control (blank) sample was used, with the larvae being kept in water with unloaded NPs under the same test conditions. All of the experiments were carried out three times, and the data were averaged.

RESULTS AND DISCUSSION

CG–MO NPs with different MO contents were obtained, with loading values from 2.6 to 4.4% MO. The characterization was performed for samples the following CG–MO ratio samples: 3 : 1, 2 : 1, and 1 : 1 loaded with 2.6; 3.5, and 4.4% MO, respectively.

Infrared spectroscopy

The CG–MO NPs were analyzed by infrared spectroscopy, with the aim of structural elucidation. Figure 1 shows the infrared spectra of CG and the CG–MO NPs. For CG, characteristic functional groups (COO— stretching) were present, with an asymmetrical band at 1660 cm^{-1} (overlapped by signals due to O—H scissor vibrations from bound water molecules) and a narrower symmetrical band at 1400 cm^{-1}. An even broader absorption was observed near 1060 cm^{-1}, which could be attributed to the COH stretching vibrations of C—O—C from glucosidic bonds and the

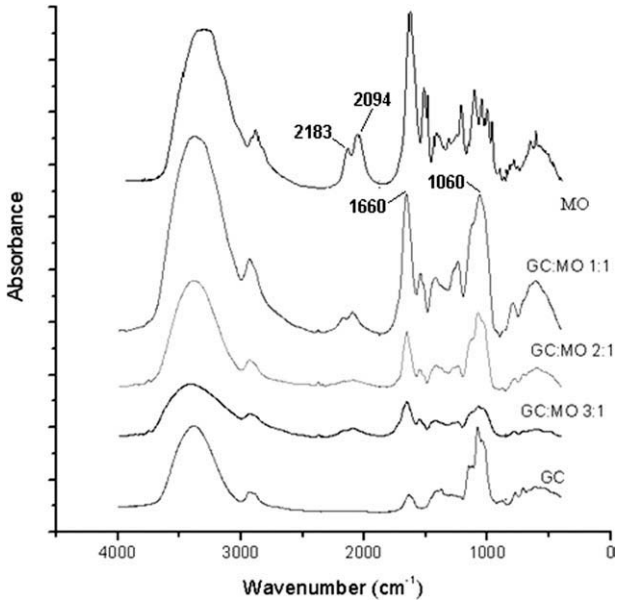

Figure 1 Infrared spectra of CG and 3 : 1, 2 : 1, and 1 : 1 CG–MO NPs.

O—H bending of alcohols.[29] The MO active principle possesses isothiocyanate groups (—N=C=S) according to the literature,[19,30] presenting corresponding absorptions at 1238 cm^{-1} (C=S) and 2182 and 2092 cm^{-1} (isocyanate asymmetric stretching).

The CG–MO NPs showed a combination of these vibration modes; when the MO content in the NPs increased, there was a sharpening of the bands at 1660 cm^{-1} and an increase in the intensities of the bands at 1238, 2182, and 2092 cm^{-1}, particularly for the CG–MO 1 : 1 sample; this confirmed the presence of the entrapped active principle.

NP size distribution

The loading, EE, ζ potential, particle size distribution, and polydispersity index (PDI) for the NPs are given in Table II. The average size of the CG–MO NPs ranged from 288 to 357 nm, and all samples exhibited unimodal distribution, as shown in Figure 2. The particle size changed with MO content, with the largest particle being obtained for the CG–MO 1 : 1 sample.

The ζ potentials of the pure components and the CG–MO NPs were determined and are shown in Table II. Pure CG presented a negative ζ potential (−8.1 ± 0.2 mV), likely because of the presence of carboxylic acid groups in the carboxylated form (COO—) in its structure. The pure MO aqueous extract presented a positive ζ potential value (+9.9 ± 0.3 mV). This extract was also spray-dried (without CG); this resulted in a sample with a negative value (−3.4 ± 0.3 mV) for its ζ potential. This indicated some kind of degradation of the compound

TABLE II
Loading, Encapsulation Efficiency, ζ Potential, Particle Size, and PDI Values for the CG–MO NPs

Sample	Loading (%)	Encapsulation efficiency (%)	ζ potential (mV)	Particle size (nm)	PDI
CG–MO 1 : 1	4.4 ± 0.4	57.8	+9.7 ± 0.2	357 ± 47	0.334 ± 0.03
CG–MO 2 : 1	3.5 ± 0.1	51.1	+7.6 ± 0.6	332 ± 30	0.367 ± 0.01
CG–MO 3 : 1	2.6 ± 0.2	39.1	+7.5 ± 0.4	288 ± 61	0.354 ± 0.03

during the spray-drying process. In addition to that, the spray-dried MO extract did not exhibited larvicidal activity, as revealed by the data from the bioassays (data not shown) and as also reported by Ferreira et al.[15]

On the other hand, the ζ potential of the CG–MO NPs assumed positive values for all formulations (from +7.5 to +9.7 mV). This seemed to be a clear indication that the entrapment of the MO active principle by spray-drying with CG as the polymeric matrix was successful, and the properties of the active substance present in the MO extract were preserved. Moreover, the positive values of the CG–MO complex indicated the formation of NPs with a core–shell structure, where the positive groups present in the MO aqueous extract interacted with the negative carboxylated groups present in the CG polymeric network, with CG chains as the core and the MO extract situated mainly in the outer shell around the core, bonded by ionic interactions and by hydrogen intermolecular interactions, as shown schematically in Figure 3.

Thermal stability

CG and the CG–MO NPs were evaluated by DSC, and the data can be seen in Figure 4(A). CG showed an endothermic peak at 89°C, which corresponded to the loss of water, and exothermic peaks at 248 and 309°C due to the decomposition processes. These temperatures were higher than those previously reported by Mothe and Rao.[31] The CG–MO NPs presented a shift in the degradation temperature toward lower values with an increase in the MO content in the NPs. This seemed to point to some sort of interaction between the CG and MO molecules, which ultimately led to a decrease in the CG thermal stability.

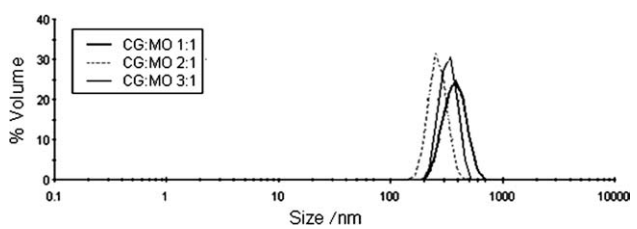

Figure 2 Particle size distribution for the CG–MO NPs.

Thermogravimetric curves of the CG–MO NPs are displayed in Figure 4(B). The samples exhibited different degradation profiles as a function of the relative MO content, whereby their thermograms exhibited four main decomposition events. The initial event was associated with water evaporation, followed by three characteristic events. The degradation of CG occurred at temperatures above 280 and 337°C and were associated with the depolymerization with the formation of water, CO, and CH_4, as reported in the literature.[29,32] The temperature decomposition for each event and the associated residual mass for the CG–MO NPs are given in Table III.

It was revealed that with increasing MO content in the formulation, there occurred a shift in the temperature decomposition of the second event from 210 to 203°C and of third event from 289 to 280°C; this was an indication of a likely interaction between MO and CG. As reported in the literature, pure CG yielded a 2.2% residual mass at 600°C.[32] The CG–MO NPs presented an increase in the residual mass at 600°C with increasing MO in the NPs, with values from 4.7 to 27.8%. CG NPs grafted with PAA (Polyacrylamide) chains[28] also presented a higher residual mass than the starting CG.

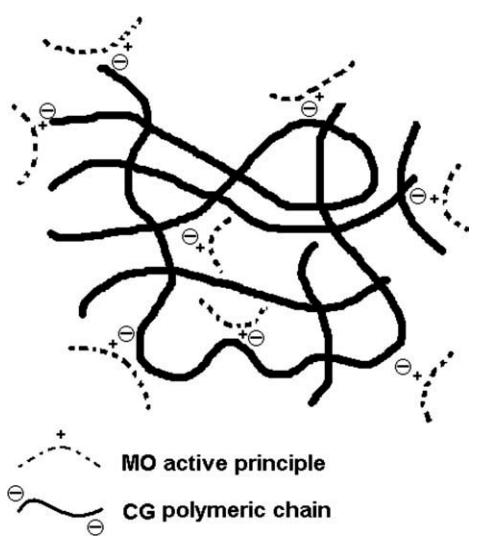

Figure 3 Proposed core–shell structure of the CG–MO NPs.

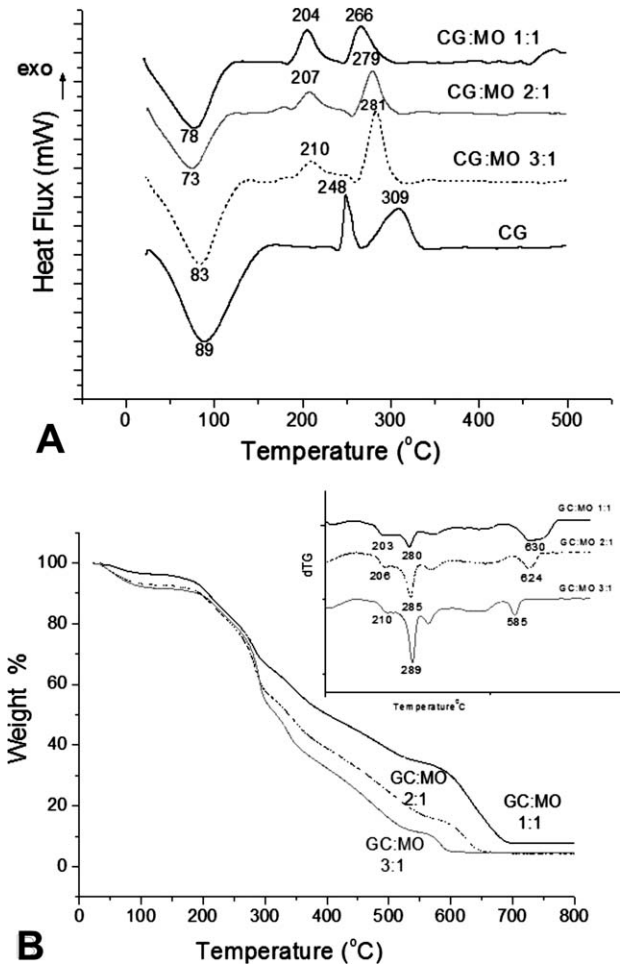

Figure 4 TGA and DSC thermograms for the CG and CG–MO NPs. dTG- Differencial Thermogravimery.

In vitro release

The CG–MO NPs presented different values of loading and encapsulation efficiency, as listed in Table II. It was observed that high MO loading led to high EE, where sample CG–MO 1 : 1 presented the highest value for EE.

In vitro kinetic studies were carried out for this sample and the CG–MO 2 : 1 sample, and the data are shown in Figure 5. The release profile of the NPs

TABLE III
Weight Losses and Corresponding Temperatures for the CG–MO NPs

	Endothermic		Exothermic	
Sample	Temperature (°C)	ΔH (J)	Temperature (°C)	ΔH (J)
CG–MO 1 : 1	74.8	0.75	207.6	0.11
			279.3	0.24
CG–MO 2 : 1	77.4	0.89	205.1	0.17
			265.3	0.18
CG–MO 3 : 1	84.5	1.16	209.3	0.07
			283.4	0.30

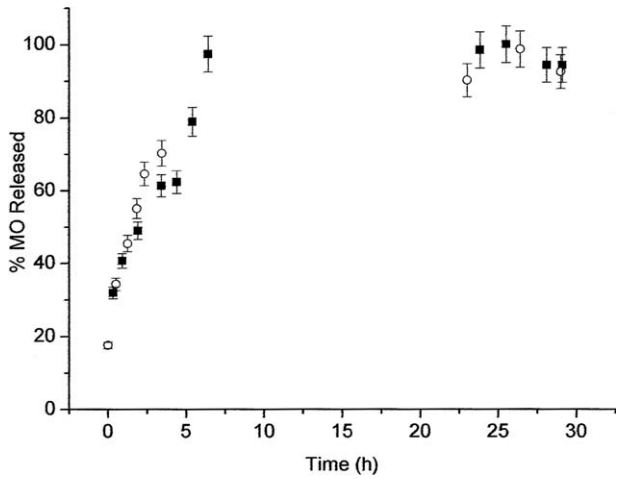

Figure 5 *In vitro* release profile for the (■) 1 : 1 and (○) 2 : 1 CG–MO NPs.

indicated that the entrapment and protection of MO was successful and that the system could effectively sustain MO release under the test conditions. The sustained release was important because of the increase of the active principle availability, which prolonged the larvicide effect. The data revealed that the CG–MO 1 : 1 and CG–MO 2 : 1 samples exhibited similar prolonged release profiles, with a steady state being achieved by 20 h for both NPs, where more than 90% of the active principle was liberated after that time period. The release parameters were determined with eq. (3):

$$M_t/M_\infty = Kt^n \tag{3}$$

where M_t is the amount of active principle at time t, M_∞ is the total amount of substance at equilibrium; M_t/M_∞ denotes the fraction of active principle released, t is the release time, and K represents a constant characteristic of the system. The diffusion exponent (n) is an indication of the mechanism of molecule release and takes values depending on the geometry of the release device.[5,7,11] A plot of $\ln(M_t/M_\infty)$ against $\ln t$ provides a linear equation [eq. (4)], whose angular coefficient is n and the linear coefficient is K. Table IV shows the obtained data:

$$\ln M_t/M_\infty = \ln K + n \ln t \tag{4}$$

In both cases, the n values were lower than 0.5; this corresponded to Fickian behavior (case I

TABLE IV
Values of the Release Kinetic Parameters n and K Obtained for the CG–MO NPs

Sample	K	n	R^2
CG:MO 2:1	0.3860	0.37	0.992
CG:MO 1:1	0.4502	0.28	0.987

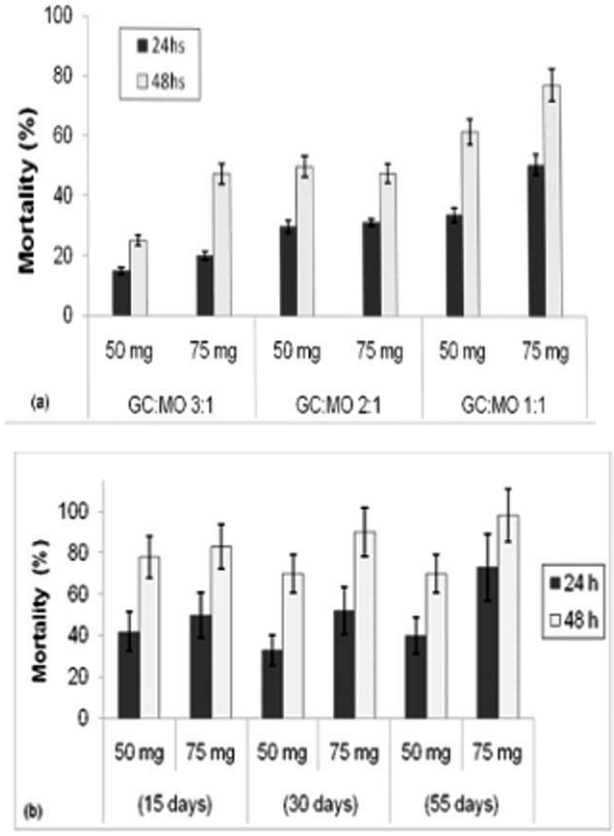

Figure 6 Mortality kinetics for the (a) CG–MO NPs and (b) CG–MO 1 : 1 sample after 15, 30, and 55 days of sample preparation.

transport), the release being dictated by a diffusional process. Polysaccharide NPs have also been used for essential oil encapsulation,[33] where the *n* exponent was reported to be equal to 1.1, which corresponded to non-Fickian behavior (case II transport), where the release could be associated with a relaxation constant.

Bioassay

The CG–MO NPs were evaluated with regard to their mortality kinetics against third instar *S. aegypti* larvae, as shown in Figure 6. It could be seen that the increase in the larval mortality was proportional to the NP content. The formulations showed different larvicidal activities according to the CG–MO relative ratio and the NP content. The CG–MO 1 : 1 NPs showed a more effective larvicide effect, with 62 ± 4 and 78 ± 3% mortality after 48 h with 50 and 75 mg of the sample, respectively. The corresponding active principle concentrations were 44 and 66 mg/L, respectively. To compare these data with figures obtained with pure aqueous MO extract, a test conducted with the MO pure extract (29 μg/mL) led to 100% mortality after 15 h (data not shown). However, the MO active principle was very unstable and easily degraded, presenting a continued loss of the larvicide effect at longer periods of time.

The preservation of the MO active principle entrapped in the CG NPs was also evaluated by a mortality kinetic bioassay for the CG–MO 1 : 1 sample after 15, 30, and 55 days of NP preparation, as shown in Figure 6(b). The mortality was evaluated at 24- and 48-h time intervals. The data revealed that the NPs presented similar mortality kinetics after 30 days of sample preparation, with an increased mortality effect (98%) even after 55 days, after being successfully preserved in the CG polymeric matrix.

CONCLUSIONS

CG–MO NPs were successfully produced by spray drying, with an operational yield of 70%. The NPs presented unimodal distribution and particle sizes ranging from 288 to 357 nm. Biopolymer CG entrapped the MO active principle and caused a protective effect, as observed by the positive values of the ζ potential of the NPs and by the decrease of the thermal decomposition temperature of CG present in the NPs. The loading and EE were proportional to the amount of MO incorporated in the NPs, with values from 2.6 to 4.4% of MO. *In vitro* release profiles for the CG–MO 1 : 1 and CG–MO 2 : 1 samples showed prolonged release with a Fickian diffusional profile. The CG–MO NPs presented an effective larvicide effect on *S. aegypti*, where the mortality rate increased according to the MO loading. In particular, the CG–MO 1 : 1 sample showed 78% mortality after 48 h. Bioassays also revealed the preservation of the active principle entrapped in the CG–MO NPs, which resulted in satisfactory mortality kinetics, even after 55 days of sample preparation.

References

1. George, M.; Abraham, T. E. J Controlled Release 2006, 114, 1.
2. Drogoz, A.; Munier, S.; Verrier, B.; David, L.; Domard, A.; Delair, T. Biomacromolecules 2008, 9, 583.
3. Kanakdande, D.; Bhosale, R.; Singhal, R. S. Carbohydr Polym 2007, 67, 536.
4. Magalhães, G. A., Jr.; Santos, C. W. S.; Silva, D. A.; Maciel, J. S.; Feitosa, J. P. A.; Paula, H. C. B.; Paula, R. C. M. Carbohydr Polym 2009, 77, 217.
5. Maciel, J. S.; Paula, R. C. M.; Paula, H. C. B.; Miranda, M. A. R.; Sasaki, J. M. J Appl Polym Sci 2006, 99, 326.
6. Jafari, S. M.; He, Y.; Bhandari, B. Dry Technol 2007, 25, 1069.
7. Paula, H. C. B.; Paula, R. C. M.; Bezerra, S. K. F. J Appl Polym Sci 2006, 102, 400.
8. Paula, R. C. M.; Heatley, F.; Budd, P. B. Polym Int 1998, 45, 27.
9. Paula, H. C. B.; Paula, R. C. M.; Gomes, F. J. S. Carbohydr Polym 2002, 48, 313.
10. Guilherme, M. R.; Reisa, A. V.; Takahashia, S. H.; Rubira, A. F.; Feitosa, J. P. A.; Muniz, E. C. Carbohydr Polym 2005, 61, 464.
11. Kulkarni, A. R.; Soppimath, K. S.; Aminabhavi, T. M.; Mehta, M. H.; Dave, A. M. J Appl Polym Sci 1999, 73, 2437.

12. Soppirmath, K. S.; Aminabhavi, T. M. Eur J Pharm Biopharm 2002, 53, 87.
13. Sá, R. A.; Santos, N. D. L.; Silva, C. S. B.; Napoleão, T. H.; Gomes, F. S.; Cavada, B. S.; Coelho, L. C. B. B.; Navarro, D. M. A. F.; Bieber, L. W.; Paiva, P. M. G. Comp Biochem Physiol C 2009, 149, 300.
14. Camurça-Vasconcelos, A. L. F.; Bevilaqua, C. M. L.; Morais, S. M.; Maviel, M. V.; Costa, C. T. C.; Macedo, I. F.; Oliveira, L. M. B.; Braga, R. R.; Silva, R. A.; Vieira, L. S. Vet Parasitol 2007, 148, 288.
15. Ferreira, P. M. P.; Carvalho, A. F. U.; Farias, D. F.; Cariolano, N. G.; Melo, V. M. M.; Queiroz, M. G. R.; Martins, A. M. C.; Machado-Neto, G. An Acad Bras Cienc 2009, 81, 207.
16. Carvalho, A. F. U.; Melo, V. M. M.; Craveiro, A. A.; Machado, M. I. L.; Bantim, M. B.; Carvalho, E. F. R. Mem Inst Oswaldo Cruz 2003, 98, 569.
17. Chuang, P. H.; Lee, C. W.; Chou, J. Y.; Murugan, M.; Shieh, B. J.; Chen, H. M. Bioresour Technol 2007, 98, 232.
18. Abdulkarim, S. M.; Long, K.; Lai, O. M.; Muhammad, S. K. S.; Ghazali, H. M. Food Chem 2005, 93, 253.
19. Sousa, M. P.; Matos, M. E. O.; Matos, F. J. A.; Machado, M. I. L.; Craveiro, A. A. In Constituintes Químicos Ativos e Propriedades Biológicas de Plantas Medicinais Brasileiras, 2nd ed.; Matos, F. J. A., ed.; Federal University of Ceará: Fortaleza, CE, Brazil, 2004.
20. Ali, G. H.; El-Taweel, G. E.; Ali, M. A. Int J Environ Studies 2004, 61, 699.
21. Pessoa, C.; Costa-Lotufo, L. V.; Leyva, A.; de Moraes, M. E. A.; de Moraes, M. O. Adv Phytomedicine 2006, 2, 197.
22. Katre, U. V.; Suresh, C. G.; Khan, M. I.; Gaikwad, S. M. Int J Biol Macromol 2008, 42, 203.
23. Eilert, U.; Wolters, B.; Nadrtedt, A. Planta Med 1981, 42, 55.
24. Guevara, A. P.; Vargas, C.; Sakurai, H.; Fujiwara, Y.; Hashimoto, K.; Maoka, T.; Kozuka, M.; Ito, Y.; Tokuda, H.; Nishino, H. Mutat Res 1999, 440, 181.
25. Oluduro, O. A.; Aderiye, B. I.; Connolly, J. D.; Akintayo, E. T.; Famurewa, O. Folia Microbiol 2010, 55, 422.
26. Santos, A. F. S.; Luz, L. A.; Argolo, A. C. C.; Teixeira, J. A.; Paiva, P. M. G.; Coelho, L. C. B. B. Process Biochem 2009, 44, 504.
27. Coelho, J. S.; Santos, N. D. L.; Napoleão, T. H.; Gomes, F. S.; Ferreira, R. S. Chemosphere 2009, 77, 934.
28. Zingali, R. B.; Coelho, L. C. B. B.; Leite, S. P.; Navarro, D. M. A. F.; Paiva, P. M. G. Chemosphere 2009, 77, 934.
29. Silva, A. D.; Feitosa, J. P. A.; Paula, H. C. B.; de Paula, R. C. M. Mater Sci Eng C 2009, 29, 437.
30. Loscutoff, P. W.; Wong, K. T.; Bent, S. F. J. Phys Chem C 2010, 114, 14193.
31. Mothe, C. G.; Rao, M. A. Thermochim Acta 2000, 357, 9.
32. Silva, A. D.; Feitosa, J. P. A.; Maciel, J. S.; Paula, H. C. B.; de Paula, R. C. M. Carbohydr Polym 2006, 66, 16.
33. Paula, H. C. B.; Sombra, F. M.; Abreu, F. O. M. S.; de Paula, R. C. M. J Braz Chem Soc 2010, 21, 2359.